An improved microfluidics approach for monitoring real-time interaction profiles of ultrafast molecular recognition

Subrata Batabyal, Surajit Rakshit, Shantimoy Kar, and Samir Kumar Pal[a)]
Unit for Nano Science and Technology, Department of Chemical, Biological and Macromolecular Sciences, S. N. Bose National Centre for Basic Sciences, Block JD, Sector III, Salt Lake, Kolkata 700098, India

(Received 13 July 2011; accepted 4 April 2012; published online 23 April 2012)

Our study illustrates the development of a microfluidics (MF) platform combining fluorescence microscopy and femtosecond/picosecond-resolved spectroscopy to investigate ultrafast chemical processes in liquid-phase diffusion-controlled reactions. By controlling the flow rates of two reactants in a specially designed MF chip, sub-100 ns time resolution for the exploration of chemical intermediates of the reaction in the MF channel has been achieved. Our system clearly rules out the possibility of formation of any intermediate reaction product in a so-called fast ionic reaction between sodium hydroxide and phenolphthalein, and reveals a microsecond time scale associated with the formation of the reaction product. We have also used the developed system for the investigation of intermediate states in the molecular recognition of various macromolecular self-assemblies (micelles) and genomic DNA by small organic ligands (Hoechst 33258 and ethidium bromide). We propose our MF-based system to be an alternative to the existing millisecond-resolved "stopped-flow" technique for a broad range of time-resolved (sub-100 ns to minutes) experiments on complex chemical/biological systems.
 [http://dx.doi.org/10.1063/1.4704839]

INTRODUCTION

In recent years, microfluidics (MF) is finding its way in more and more practical applications in a vast majority of fields including physics, biology as well as in many chemical applications such as separation of products, polymerase chain reactions, etc.[1,2] During the past decade, it outweighed the traditional analytical instruments, as it provides a means for reducing both analysis time and the amount of reagents necessary to perform each analysis. Virtually, the microfluidics methodology is based on the low Reynolds number as well as the diffusion of the analytes or particles of interest.[3,4] Within the micro-channel, diffusion plays a critical role in the reaction or mixing mechanism, and proper mixing requires certain tactics[5] involving the suitable control of flow rates and the complex microfluidics geometry. One important aspect of the microfluidics methodology lies in the kinetics study of chemical and biological phenomena. Kinetics studies of fast processes in flasks are cumbersome due to the lack of homogeneity and relatively slow mixing that typify batch processes.[6–8] On the other hand, the stopped-flow method[9] has been a quite widespread technique to monitor fast chemical reactions, where the reaction is terminated at the fluidics path. The bulk approach provides the information about the end-point of reactions or interactions, but it lacks the valuable information regarding the intermediary steps. Similarly, in case of stopped-flow kinetics,[10–13] the achievable time resolution, to date, is in the order of milliseconds.[14] In contrary, in case of continuous flow microfluidics, both end-point as well as location-specific in-depth information can be obtained,[15–17] enabling to envisage and interpret reactions/interactions profiles more appropriately. The kinetic information (time scales) can be extracted through space-to-time conversion by measuring the product formation at different positions along the micro-channel.

Until now, the exploration of reaction kinetics using MF techniques essentially focuses on the ability to control the reaction, and the use of a minimum amount of reagent,[18–20] and rather less efforts have been made for the enhancement of time resolution associated with diffusion-controlled reactions.[7,21–23] However, better time resolution in such reactions is essential in order to reveal the "missing" parts in the kinetics such as the existance of intermediate states in a molecular recognition process. By thoughtful adjustment of the flow rate and geometry of the micro-channel, the reaction within MF channel initially takes place, which ensures that the extent of the reaction changes significantly from the start to the end of the flow path.[16] The reaction profile can be obtained by the quantitative comparison of the reaction product(s) or reactants themselves.[24] It is not always crucial for the reaction to be completed by the end of the micro-channel; the only prerequisite is that the selected analytical technique (e.g., fluorescence intensity,[25] decay time, fluorescence lifetime image,[15] etc.) is sensitive enough to detect the change in the product or reactant concentrations along the flow path. The present work describes the development of microfluidics as an advanced analytical platform for studying molecular interactions or even very fast chemical reactions. The use of time-resolved fluorescence spectroscopy as well as fluorescence microscopy enables us to follow the reaction kinetics with better time resolution revealing the intermediate states of molecular recognition and providing a way to correlate different sets of experimental data. The special design of the flow channel enables it to withstand higher flow rates (~14 ml/min) without any leakage or turbulence and a specifically small region of the

a)Author to whom correspondence should be addressed. Electronic mail: skpal@bose.res.in.

micro-channel serves the purpose of achieving significantly higher time resolution. The developed platform is capable of providing a time resolution as good as sub-hundred nanoseconds with the suitable adjustment of flow rates, which is not possible to achieve with existing stopped-flow techniques. As demonstrated with a fast ionic reaction between sodium hydroxide and phenolphthalein, microsecond-resolved kinetics was observed. The same MF platform also serves the purpose of a stopped-flow method as the flow velocity can be brought to zero after which the diffusion process can be followed. The process is the reverse of the existing stopped-flow techniques and can be termed as "flow-stopped" method. It provides an efficient way for studying diffusion-controlled phenomena such as energy/charge transfer in biomolecular interactions. We have further applied our MF system to the investigation of intermediate states involved in the molecular recognition of macromolecular self-assemblies (micelles with different charges) and genomic DNA (from salmon testes) by small ligands (Hoechst 33258 and ethidium bromide (EtBr)).

MICROFLUIDICS PLATFORM AND ANALYTICAL APPROACH

Device design

Figure 1(a) portrays the used MF system, represented as the Y-shaped MF chip. The specially designed MF chip with the connectors and the syringe pumps (Atlas-ASP011) were from Dolomite, UK and Syrris Ltd., UK, respectively. The specially designed MF chip consists of two inlets and a common outlet. The chip was made out of optically transparent glass, which can sustain higher temperature if required. The diameter of the microchip (440 μm) was designed to withstand high flow rates. A small special region just after the confluence (Figure 1(a): X region) with a diameter of 150 μm and a length scale around 2200 μm

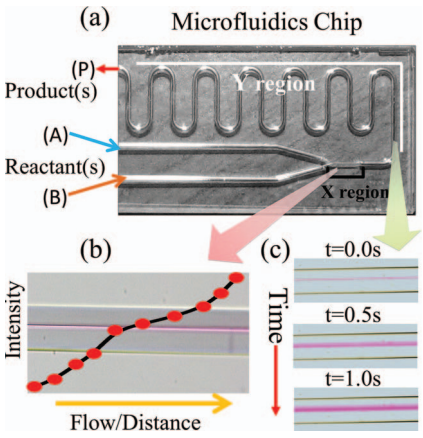

FIG. 1. (a) Specially designed microfluidics chip for the measurement of ultrafast kinetics. Two specific regions are shown: X, for fast sub-100 ns kinetics and Y, for slower kinetics. (b) A fast ionic model reaction between sodium hydroxide and phenolphthalein measured in the microfluidics chip (X region) on the microsecond time scale is shown. (c) The "flow-stopped" methodology applied to the same ionic reaction at a fixed position (Y region) of the micro-channel without any flow of the reactants is shown. The snapshots reveal the role of diffusion in the ongoing reaction (see text).

was deliberately added in the design, after which it expands to 440 μm (Figure 1(a): Y region). The small diameter guarantees a higher fluid front velocity with reasonably low Reynolds number. The special geometry empowers to study very fast kinetics with a time resolution in the order of nanoseconds. For the study of slow kinetics in the range of millisecond to microsecond, the other portion of the micro-channel with a diameter of 440 μm is suitable. The two inlets were attached to a syringe pump by capillary tubes. The capillaries were passed through the shaft of the holder prior to connection with the MF chip. The reagents were propelled using the syringe pump and the total volumetric flow rate was adjusted according to the requirements. In the sections "results and discussion," and "conclusion," the term "flow rate" refers to the combined volumetric flow rate of the reagents through the micro-channel. The schematic of the MF channel is presented as a tube with a cross section S, length L, and total volume V = SL (Figure 2(a)). The streams converge and their mixing starts in the micro-channel junction, position X_0 in the Figure 2(a). The total length of the flow path of the micro-channel is around 10 cm.

Fluorescence detection

Fluorescence images were captured with a fluorescence microscope (BX-51, Olympus America Inc.) equipped with a 100 W mercury arc lamp, which was used as the excitation source (UV light excitation) and a DP72 CCD camera (Figure 2(b)). The excitation light was cutoff by using a standard filter and the fluorescence was collected through a 10× objective. The image processing and analysis were done by the "ANALYSIS" software provided with the microscope. A region of interest (ROI) was selected at a specific height and width. This ROI was used to obtain an intensity profile along the micro-channel. Intensity profiles were acquired at a particular micro-channel distance from the initial mixing confluence. The red-green-blue (RGB) analysis was performed wherever required. This channel distance was converted into the reaction time (t_n) by dividing it by the velocity of the flow (U (m/s)), obtained from the known volumetric flow rate and cross section (S) of the micro-channel.

Time-resolved studies

For the time-resolved measurements, a platform was developed to combine the micro-channel with picoseconds pulsed laser light (Figure 2(c)). The fluorescence transients on the microchip were measured with a commercially available spectrophotometer (Life-Spec-ps) from Edinburgh Instrument, UK. The MF platform was held by a homemade translation stage moveable in XY and XZ directions. The arrangement enables the collection of fluorescence transients at different positions along the channel (Figure 2(c)) with precision and accuracy. The angle of the fluidics chip was optimized in order to collect the maximum number of photons on the detector and to achieve a reasonable stop rate. A picosecond pulsed laser diode was used to excite the sample at 375 nm (instrument response

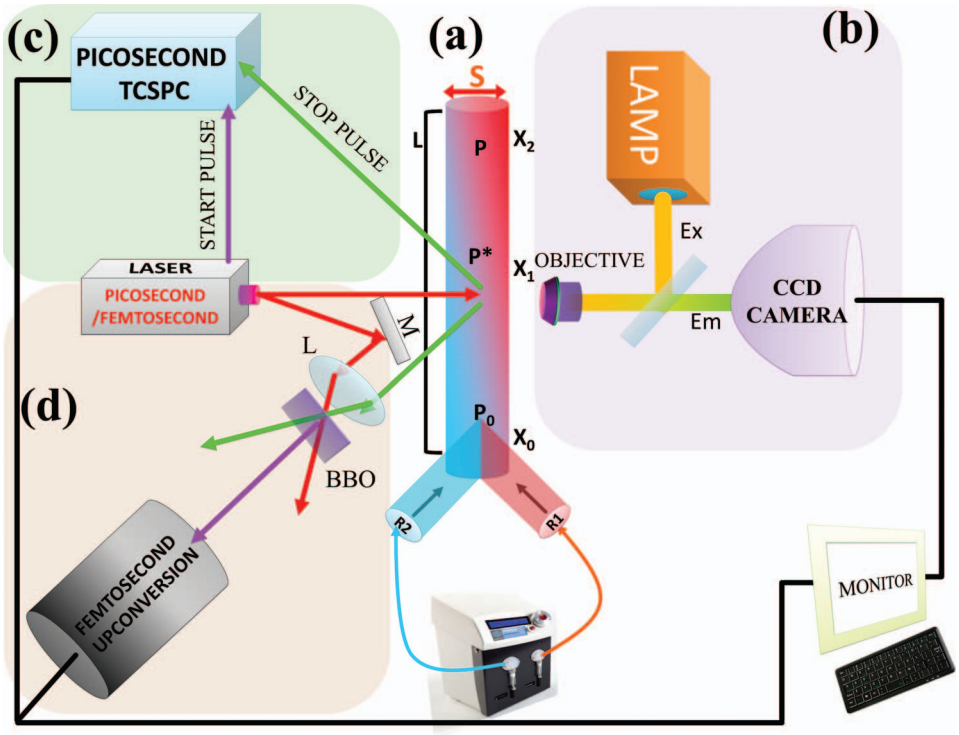

FIG. 2. (a) Schematic presentation of the developed microfluidics platform. L denotes the flow path length, X_i are the positions for measurements along the channel, and S is the cross section of the micro-channel. (b) The fluorescence microscope coupled to the microfluidics channel. A CCD camera captures images of the ongoing reactions inside the micro-channel. (c) Picosecond-resolved fluorescence technique (TCSPC) for the collection of decay profiles along the micro-channel. (d) Femtosecond upconversion technique combined with the microfluidics platform for studying ultrafast dynamics.

function (IRF) of 60 ps). The excitation was vertically polarized, and the emission was recorded through a polarizer oriented at 55° from the vertical position. Incorporation of a long-pass filter with a cutoff at 395 nm in the emission channel effectively eliminates possible scattered excitation light. As for the study of very fast dynamical time scale (∼femtosecond), the arrangement was made as depicted in Figure 2(d). In order to couple a femtosecond-resolved upconversion setup with our MF system, a homemade micrometer translation stage has been used.

Materials used

Hoechst 33258 ((2′-4-hydroxyphenyl)-5-(4-methyl-1-1-piperazinyl)-2,5′-bis-1H-benzimidazole, tris-hydrochloride) and ethidium bromide (3,8-Diamino-5-ethyl-6-phenyl-phenanthridinium bromide) were obtained from Molecular Probes. Salmon sperm DNA was purchased from Sigma. Sodium dodecyl sulphate (SDS) and cetyl trimethyl ammonium bromide (CTAB) were obtained from Fluka, and TX-100 was purchased from ROMIL. Sodium hydroxide and phenolphthalein were purchased from Merck. The chemicals were of highest commercially available purity and were used as received. Aqueous solutions were prepared in the phosphate buffer (100 mM). The stock solution of DNA was prepared by dissolving the lyophilized powder of salmon sperm DNA into the phosphate buffer. The concentration of the dye in aqueous solution was estimated by taking the extinction coefficient value of 46 000 $M^{-1}cm^{-1}$ at 345.5 nm for H33258 and 5680 $M^{-1}cm^{-1}$ at 476 nm for EtBr. Throughout the experiments, fluoroprobes concentrations were kept below 50 μM and micellar concentrations were kept around 1 mM. To increase the signal strength, the concentrations of the ligand fluoroprobes were optimized as described above.

Interpretation of the kinetics

The kinetics data for the reaction between sodium hydroxide and phenolphthalein were analyzed by considering the colour intensity (pink) of the anionic species formed during the reaction. For the molecular recognition, the kinetic parameters were determined by measuring the fluorescence intensity at different positions along the channel as the reaction progresses and changes in the fluorescence intensity were used as a marker of the interaction. The time-resolved studies in case of H33258 also provided a qualitative indication of the kinetics involved.

The model reactions that have been studied in our MF channel are well documented in the literature and found to follow first-order kinetics.[26–28]

For a single step first-order reaction, reactants will produce products as follows:

$$\text{Reactants} \xrightarrow{k} \text{Products}$$

The rate equation can be written as,[29]

$$x = a(1 - e^{-kt}), \tag{1}$$

where, "x" corresponds to the product concentration at time t and k is the first-order rate constant.

Considering a reaction having an intermediate step, i.e., $A \xrightarrow{k_1} I \xrightarrow{k_2} P$, the product concentration at time, t would be,[29]

$$x = a\left(1 + \frac{k_1 e^{-k_2 t} - k_2 e^{-k_1 t}}{k_2 - k_1}\right), \qquad (2)$$

where, "a" denotes the initial concentration at time t = 0 and k_1, k_2 are the respective rate constants.

The precision of the measurement of the kinetics parameter will depend on the uniformity and accuracy of the flow velocity and the signal-to-noise ratio in the fluorescence measurement. Particular care needs to be taken in these respects. In order to maintain uniform flow velocity, we have employed a high precision injection pump. To achieve a better fluorescence signal-to-noise ratio, relatively high concentrations of the fluorescent probes were used. Reproducibility of the measured rate constant values within 5% error range indicates the precision of our technique.

RESULTS AND DISCUSSION

In order to study a fast model reaction in our MF device, we have chosen the ionic reaction of sodium hydroxide with phenolphthalein ($H_2P_{(aq-colourless)} + 2OH^- \rightarrow P^{2-}_{aq-pink} + 2H_2O$). The flow rate of 7 ml/min for each channel, i.e., 14 ml/min of overall fluid front velocity in the MF channel leading to a spatial resolution of 70 ns/μm, does not reveal any detectable reaction product ($P^{2-}_{aq-pink}$) in the channel, even at the end of the small channel (Figure 1(a): X region). The observation clearly shows that the formation of product is negligible even after 165 μs of confluence. However, the flow rate of 500 μl/min in each channel, leading to a spatial resolution of 1 μs/μm clearly reveals the formation of the anionic pink species (Figure 1(b)). The intensity of the anionic pink species increases steadily along the micro-channel. The pseudo-first-order rate constant was estimated to be 3.2×10^{-4} s^{-1}, which is almost similar to the reported literature value (0.7×10^{-4} s^{-1}).[30] Figure 1(c) reveals the MF platform for studying diffusion-controlled reactions without any external velocity components, i.e., essentially as in the flow-stopped method, for the same reaction as described above. The intensity as well as the width of the product zone increases with time, enabling to visualize the diffusion process. The method is found to be very efficient for studying diffusion-controlled biological phenomena such as energy/charge transfer processes in protein-protein and protein-DNA interactions. Recently, we have explored[31] the time scales associated with the biomolecular recognition of a DNA-binding λ-repressor protein with operator DNA (O_R1) using these techniques.

In order to study the time-resolved reaction pathways associated with the molecular recognition (complexation) with self-assembled anionic SDS micelles by a cationic ligand Hoechst 33258 (H33258), we have used fluorescence microscopy and picosecond-resolved emission spectroscopy with our MF device (Figure 2). It has to be noted that anionic micelles are good mimics of DNA,[32] having a negatively charged surface and hydrophobic interior. The cationic ligand

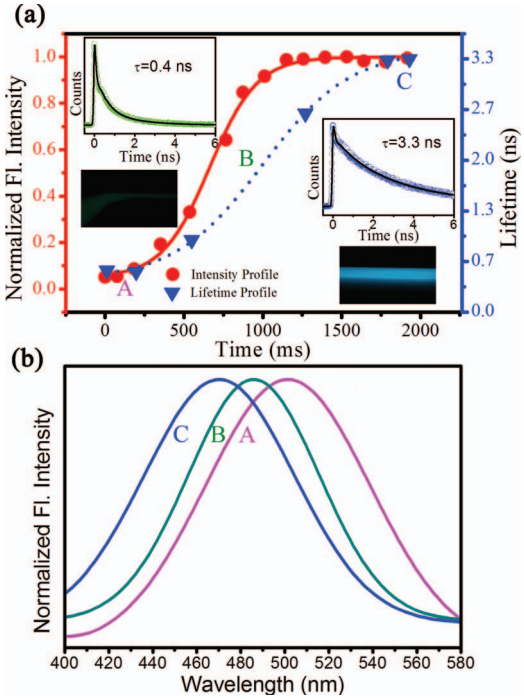

FIG. 3. (a) Fluorescence intensity profile of H33258 in the complexation reaction with SDS (red dots). Fluorescence images showing the extent of the reaction along the microfluidics channel as revealed by the increase in fluorescence intensity and change in the fluorescence maximum (inset images). Picosecond-resolved fluorescence transients of H33258 (inset traces) depicting the dynamical lifetime of H33258 along the channel (blue triangles). Solid and dotted lines indicate the fit of the experimental data with the appropriate kinetic equation as described in the text. (b) Depicts the change in the fluorescence emission maximum in the course of the complexation. A, B, and C denotes three positions along the micro-channel as shown in the upper panel of the figure. The emission maximum is blue shifted from 500 nm (A), to 485 nm (B), and finally to 470 nm (C).

H33258 is a well-known DNA minor groove binder,[33] which reveals significantly higher fluorescence yield in hydrophobic environments compared to that in bulk water. It has earlier been shown that H33258 remains at the interface of the SDS micelles projecting its cationic charges toward the anionic SDS head groups and the bis-benzimidazole moiety at the hydrophobic side.[33] In this regard, the molecular recognition of SDS micelles by H33258 is expected to be interesting, as there are two possible ways of complexation. H33258 may directly approach the micelle and form the complex (single step), or the ligand may form an intermediate complex with the micelle via electrostatic interaction, and finally form the energy minimized complex as revealed in equilibrium (two steps). Figure 3(a) displays the interaction profile of H33258 with SDS micelle based on the detected fluorescence images as well as fluorescence transients along the channel at desired specific locations. The overall flow rate was kept at 150 μl/min. In Figure 3(a), the numerical fit of the fluorescence intensity (red solid line) according to equation (2) is reasonably good, indicating the reaction pathway to be a two-step process (Figure 6(a)).[34] The overall rate constant of the interaction profile was estimated to be 2.1 s^{-1}. The fluorescence lifetime of H33258 increases (0.4 ns to 3.3 ns) along the micro-channel and the pattern is consistent with the increase of fluorescence intensity value as well as the change in

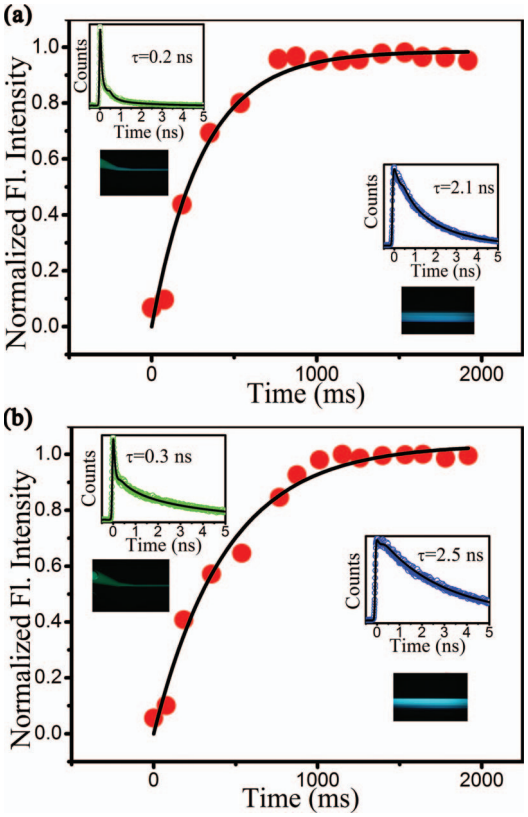

FIG. 4. Fluorescence intensity profile of H33258 in the complexation reaction with CTAB (a) and TX100 (b), respectively. Fluorescence images (insets) showing the extent of the reaction along the microfluidics channel as revealed by the increase in fluorescence intensity. Picosecond-resolved fluorescence transients of H33258 (inset traces) depicting the dynamical lifetime of H33258 along the channel during the complexation.

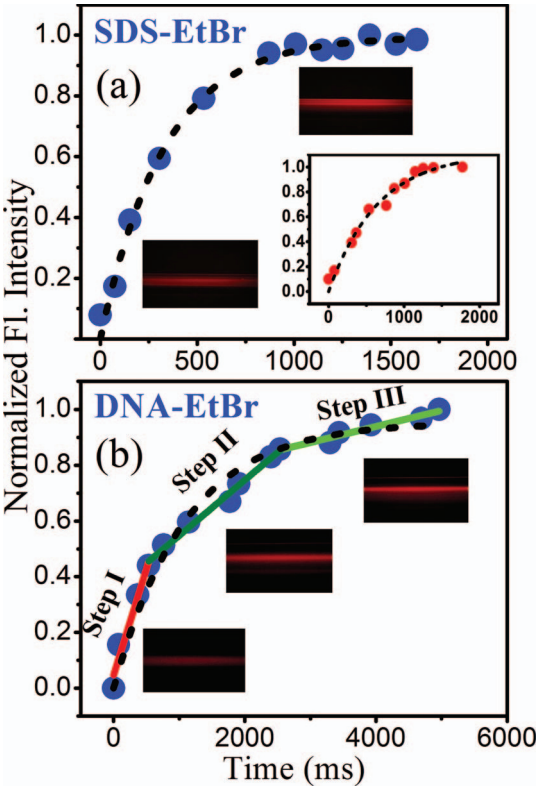

FIG. 5. Fluorescence intensity profile of EtBr along the micro-channel as obtained from the fluorescence microscope. The complexation of the probe EtBr with the SDS micelle (a) and the three step intercalation process of the probe into the DNA (b) are shown. Dashed lines indicate the fits of the experimental data (dots) to the appropriate kinetic equations as described in the text. The inset of (a) depicts the fluorescence intensity profile of EtBr-TX100 complexation.

emission maximum (500 nm to 470 nm, emission maximum is blue shifted as indicated in Figure 3(b)).

The reported lifetime value of H33258 in buffer is ~300 ps,[15] which is similar to the value obtained at the mixing point of the Y junction (Figures 1(a) and 2(a)). The observation reveals insignificant interaction of H33258 with the SDS micelle at the mixing point (X_0 of Figure 2(a)). At the saturation point of the reaction profile of H33258-SDS binding, the lifetime value of H33258 is measured to be 3.3 ns in the MF channel, which closely resembles the lifetime of H33258 in SDS micellar environment in equilibrium.[35] We have also studied the nature of complexation of H33258 with cationic (CTAB) and neutral (TX-100) micelles as shown in Figure 4. The complexation of H33258 with the two micelles is consistent with the kinetic pathways as described in Eq. (1), which is one-step in nature (Figure 6(b)). From these studies on the complexation of H33258 with model micellar systems, interesting pathways associated with the molecular recognition of DNA in the minor groove binding[33] of H33258 can be anticipated and are in progress in our group.

In addition, we have used our developed system in order to study the molecular recognition of DNA by a well-known intercalator, EtBr. In this endeavor, we have first studied the interaction profile of EtBr with anionic SDS micelle as shown in Figure 5(a). The intensity profile of EtBr upon complexation with the micelle reasonably follows a one-step mechanism. The first-order rate constant was calculated to be 3.0 s^{-1}. In the case of the neutral TX-100 micelle, the complexation pathway is comparable to that of the SDS micelle as shown in the inset of Figure 5(a). We have observed that the emission of the cationic ligand EtBr does not change

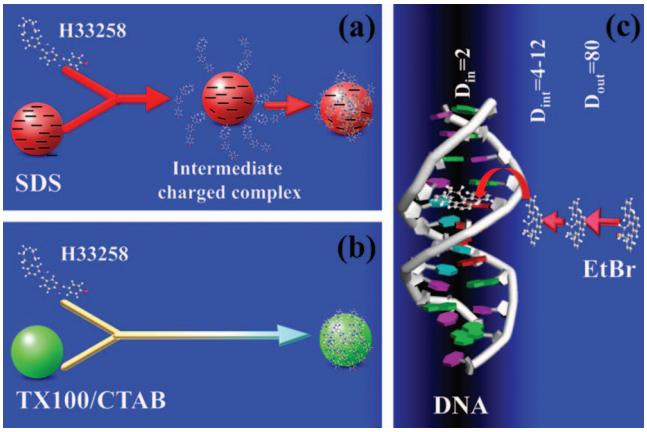

FIG. 6. (a) Schematic showing the formation of the intermediate charge complex for the molecular recognition of SDS micelles with H33258. (b) One-step molecular recognition of TX100 and CTAB micelles with H33258. (c) Schematic of DNA-EtBr interactions. D_{in}, D_{int}, and D_{out} are the dielectric values at the DNA centre, at the DNA surface and in bulk water, respectively. The scheme describes the multi-step intercalation process of EtBr into the DNA.

appreciably from that in bulk water in the presence of the cationic CTAB micelle revealing negligibly small interaction with the micelle. On the other hand, multi-step pathways involved in the complexation of EtBr with the genomic DNA are very clear from the intensity profile as shown in Figure 5(b). It has to be noted that, the enhancement of fluorescence intensity of the EtBr probe is associated with the decrease in the dielectric constant of the host medium around the probe,[36] associated with retarded proton transfer in EtBr. It has been shown that the local dielectric environment around DNA reveals a radial distribution of dielectric constants from a value of 2 at the center to 80 at 5 Å away from the DNA surface.[37] At the DNA surface, the dielectric constant is found to be around 4–12.[38] Thus, in the course of intercalation, the intercalator EtBr has to diffuse through three distinct environments with different dielectric constants as shown in Figure 6(c). Our observation of intercalation in terms of intensity enhancement of EtBr as shown in Figure 5(b) distinctly reveals three different regions. The observation is consistent with the fact that the probe EtBr has to interact with the surface of the DNA, probably making an intermediate surface adduct before the final intercalation. The overall rate constant for the DNA-EtBr interaction was estimated to be 0.9 s^{-1}, which is in reasonably good agreement with the reported value (0.7 s^{-1}).[26]

CONCLUSION

In summary, the developed MF system provides an alternative for studying complex chemical and biological systems with sub-100 ns resolution. The platform provides an alternative way for achieving a better time resolution to study very fast kinetics. The incorporation of time-resolved spectroscopy further reinforces the technique to observe the decay dynamics. The successful implementation of the approach explored the complexation behavior of two drugs in bio-mimetic and biological systems. The key findings include the identification of the intermediate pathways of EtBr intercalation into DNA. The micellar systems provide a significant insight in the complexation of macromolecular recognition. Overall, our approach may be well applied to biological systems like protein-DNA, protein-protein interactions to visualize and interpret the underlying mechanism. Our microfluidic approach allows extraction of location-specific data, which in turn provides a better tool to diagnose a chemical reaction with higher time resolution.

ACKNOWLEDGMENTS

S.B., S.R., and S.K. thank Council of Scientific and Industrial Research (CSIR) for the research fellowships. We thank DST for financial grants (Grant No. SR/SO/BB-15/2007). We like to thank Dr. Renske Van Der Veen, California Institute of Technology, USA, for her critical reading of the manuscript.

[1] J. W. Hong and S. R. Quake, Nat. Biotechnol. **21**, 1179 (2003).
[2] M. G. Whitesides, Nature (London) **442**, 368 (2006).
[3] A. P. Sudarsan and V. M. Ugaz, Proc. Natl. Acad. Sci. U.S.A. **103**, 7228 (2006).
[4] T. M. Squires and S. R. Quake, Rev. Mod. Phys. **77**, 977 (2005).
[5] S. Yao and O. Bakajin, Anal. Chem. **79**, 5753 (2007).
[6] G. H. Seong and R. M. Crooks, J. Am. Chem. Soc. **124**, 13360 (2002).
[7] C. Wang, S. J. Li, Z. Q. Wu, J. J. Xu, H. Y. Chen, and X. H. Xia, Lab Chip **10**, 639 (2010).
[8] W. D. Ristenpart, J. D. Wan, and H. A. Stone, Anal. Chem. **80**, 3270 (2008).
[9] K. R. Fox and M. J. Waring, Biochemistry **23**, 2627 (1984).
[10] J. Mori, Y. Miyashita, D. Oliveira, H. Kasai, H. Oikawa, and H. Nakanishi, J. Cryst. Growth **311**, 553 (2009).
[11] J. Alves, C. Urbanke, A. Fliess, G. Maass, and A. Pingoud, Biochemistry **28**, 7879 (1989).
[12] J. Jiang, J. F. Bank, and C. P. Scholes, J. Am. Chem. Soc. **115**, 4742 (1993).
[13] T. D. Pollard, P. Maupin, J. Sinard, and H. E. Huxley, J. Electron Microsc. Tech. **16**, 160 (1990).
[14] G. Feng and T. Jia, Appl. Spectrosc. **60**, 1477 (2006).
[15] R. K. P. Benninger, O. Hofmann, B. Önfelt, I. Munro, C. Dunsby, D. M. Davis, M. A. A. Neil, P. M. W. French, and A. J. Mello, Angew. Chem., Int. Ed. **46**, 2228 (2007).
[16] S. Mozharov, A. Nordon, D. Littlejohn, C. Wiles, P. Watts, P. Dallin, and J. M. Girkin, J. Am. Chem. Soc. **133**, 3601 (2011).
[17] O. Bilsel, C. Kayatekin, L. A. Wallace, and C. R. Matthews, Rev. Sci. Instrum. **76**, 014302 (2005).
[18] H. Song and R. F. Ismagilov, J. Am. Chem. Soc. **125**, 14613 (2003).
[19] Y. J. Song, J. Hormes, and C. Kumar, Small **4**, 698 (2008).
[20] A. Abou-Hassan, O. Sandre, and V. Cabuil, Angew. Chem., Int. Ed. Engl. **49**, 6268 (2010).
[21] T. Robinson, H. B. Manning, C. Dunsby, M. A. A. Neil, G. S. Baldwin, A. J. de Mello, and P. M. W. French, Proc. SPIE **7593**, 759304 (2010).
[22] H. Y. Park, S. A. Kim, J. Korlach, E. Rhoades, L. W. Kwok, W. R. Zipfell, M. N. Waxham, W. W. Webb, and L. Pollack, Proc. Natl. Acad. Sci. U.S.A. **105**, 542 (2008).
[23] H. Roder, K. Maki, and H. Cheng, Chem. Rev. **106**, 1836 (2006).
[24] C. N. Baroud, A. M. Huebner, C. Abell, W. T. S. Huck, and F. Hollfelder, Anal. Chem. **83**, 1462 (2011).
[25] T. Thorsen, S. J. Maerkl, and S. R. Quake, Science **298**, 580 (2002).
[26] C. Mandal, S. W. Englander, and N. R. Kallenbach, Biochemistry **19**, 5819 (1980).
[27] F. Bernges and E. Holler, Nucleic Acids Res. **19**, 1483 (1991).
[28] F. Garland, D. E. Graves, L. W. Yielding, and H. C. Cheung, Biochemistry **19**, 3221 (1980).
[29] K. J. Laidler, *Chemical Kinetics*, 3rd ed. (Prentice-Hall, 1987).
[30] K. Y. Tam and F. T. Chau, J. Autom. Chem. **14**, 157 (1992).
[31] T. Mondol, S. Batabyal, and S. K. Pal, "Ultrafast Electron Transfer in the Recognition of Different DNA Sequences by a DNA-binding Protein with Different Dynamical Conformations," J. Biomol. Struct. Dyn. (in press).
[32] S. Pal, P. K. Maiti, and B. Bagchi, J. Phys.: Condens. Matter **17**, S4317 (2005).
[33] D. Banerjee and S. K. Pal, Chem. Phys. Lett. **432**, 257 (2006).
[34] T. D. Slavnova, A. K. Chibisov, and H. Gorner, J. Phys. Chem. A **109**, 4758 (2005).
[35] T. Mondol, P. Rajdev, A. Makhal, and S. K. Pal, J. Phys. Chem. B **115**, 2924 (2011).
[36] S. K. Pal, D. Mandal, and K. Bhattacharyya, J. Phys. Chem. B **102**, 11017 (1998).
[37] M. A. Young, B. Jayaram, and D. L. Beveridge, J. Phys. Chem. B **102**, 7666 (1998).
[38] J. M. Leveritt, C. Dibaya, S. Tesar, R. Shrestha, and A. L. Burin, J. Chem. Phys. **131**, 245102 (2009).